

The effect of surfactants on the particle size and optical properties of precipitated ZnO nanoparticles

Jamil Kamal Salem, Talaat Moussa Hammad

(Faculty of Science, Al-Azhar University, P.O. Box 1277, Gaza, Palestine)

Abstract: Wurtzite ZnO nanoparticles were prepared in aqueous solutions with additives of Triton (Tx-100), sodium dodecyl sulfate (SDS) and cetyltrimethyl ammonium bromide (CTAB). HRTEM micrographs and XRD of all samples are showed nearly spherical nanoparticles with average particle size of 3.4-11 nm. A significant blue shift in the excitonic absorption, for nanoparticles prepared in the presence of surfactants Tx-100 and CTAB compared to that of the ZnO nanoparticles. The particle size calculations from the absorption edge showed that ZnO nanoparticles grown with CTAB have smallest particle size and lowest Stokes shift.

Key words: nanoparticles; ZnO; surfactants; optical properties

1. Introduction

Zinc oxide (ZnO) is a wide band gap semiconductor with energy of 3.2 eV at room temperature. It is a versatile material that has achieved applications in photocatalyst, solar cells, chemical sensors, piezoelectric, transducers, transparent electrodes^[1-2], electroluminescent devices and ultraviolet laser diodes^[3-4]. Hence, investigations on the synthesis and modification of nanosized ZnO have attracted tremendous attentions. The ZnO nanocrystals always exhibit novel unique properties due to quantum confinement effects compared with their bulk properties^[5-8]. The quantum confinement of nanocrystalline ZnO particles can be illustrated from the blue shift in the photoluminescence UV emission. Nevertheless, the properties of the ZnO nanocrystals depend closely on their particle sizes, morphology, surface area and activity. Different synthesis methods

have been devised, including sol-gel technique^[9], microemulsion synthesis^[10], mechanochemical processing^[11], spray pyrolysis and drying^[12], thermal decomposition of organic precursor^[13], RF plasma synthesis^[14], supercritical-water processing^[15], self-assembling^[16], hydrothermal processing^[17], direct precipitation^[18] and homogeneous precipitation^[19]. The application of the surfactants provides a means to achieve control over the ZnO nanoparticle size and size distribution, which is essential for tailoring optical, electrical, chemical, and magnetic properties of nanoparticles for specific applications. In this study, the authors prepared ZnO nanoparticles in aqueous solutions using various additives, and investigated the effect of these additives (CTAB, SDS and Tx-100) on the morphology and size control of the ZnO nanoparticles.

2. Experiment

All the chemicals were of analytical grade and used without further purification. In the typical procedure, 100 mL of 0.05 M solution of surfactant (CTAB / SDS / Tx-100) was made in distilled water and divided into two parts. These two parts were used to prepare 0.5 M zinc acetate dehydrate and 2 M NaOH separately. The solution of NaOH was added using a drooping funnel under stirring. The stirring was continued for 2 h after the completion of addition of NaOH. The solution was left to age for 12 hrs. The solution was centrifuged to obtain the precipitate. The precipitate was washed with water and acetone to

Corresponding Author: Talaat Moussa Hammad (1957-), male, professor; research field: material science. E-mail: t.hammad@alazhar-gaza.edu.

remove the unreacted materials and organic impurities. The precursor was dried in an electric oven at 110°C. The dried product was then crushed and calcined at 200°C for 3 hrs. We have also synthesized a sample without surfactants by this method. Colloidal solution of zinc oxide in ethanol (1×10^{-3} M) has been prepared with ultrasonic for 20 mins. The UV-vis absorption spectra were taken with a Hewlett Packard8453 spectrometer of ethanolic nanoparticle solutions made by sonication of the products in ethanol. The TEM analysis was done with a Tecnai F300 transmission electron microscope, images taken after suspending the nanoparticles in 95% ethanol. Crystal structure identification and crystal size analysis were performed with an X-ray diffractometer XDS 2000, Scintac Inc., USA with $\text{CuK}\alpha$ radiation source and scan rate of $2^\circ/\text{min}$.

3. Results and discussion

3.1 Crystal structure and morphologies

Fig. 1 demonstrates the XRD profiles of the ZnO nanoparticles prepared in different surfactant solutions. The diffraction peaks of spectra all coincide with JCPDS card No. 36-1451, so that the observed patterns can be unambiguously attributed to the presence of hexagonal wurtzite crystallites. No excess peaks detected, which indicate that all the precursors have been completely decomposed and no other complex products were formed. It should be noted here that the full width at half maximum (FWHM) of the diffraction peaks changes with various additives of surfactants. Furthermore, the crystalline size can be estimated to be 12, 9, 6 and 4 nm, for pure ZnO, Tx-100, SDS and CTAB additives respectively, by using the Debye-Scherrer formula. Larger crystalline size of 12

and 9 nm was obtained for the ZnO crystals grown in the solution with additive SDS, respectively. On the other hand, in cases of SDS and CTAB, the ZnO crystals show smaller crystalline size of 6 and 4 nm. The difference in the estimated crystalline size indicates that there are some differences in size and morphology of the ZnO crystals.

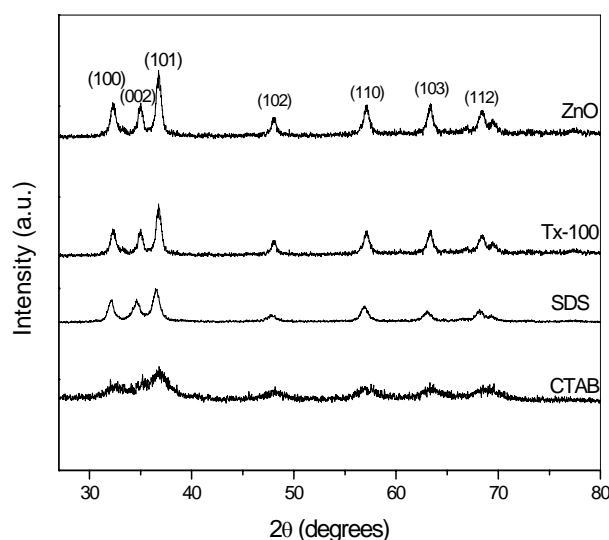


Fig. 1 XRD patterns of the products grown in the solutions with various additives

Note: In all cases, all the peaks can be indexed as wurtzite ZnO.

Fig. 2 represents the HRTEM micrographs and histograms of ZnO nanoparticles prepared in different surfactant solutions. HRTEM micrographs of all samples are showed nearly spherical nanoparticles with average particle size of 3.4-11 nm. The HRTEM micrographs indicate that the ZnO nanoparticles prepared in different surfactants solutions didn't control the shape of ZnO but their particle sizes. The ZnO crystals grown with CTAB show smaller average size (3.4 nm). The results suggest that by using surfactants, morphology of ZnO can't be changed in precipitation process.

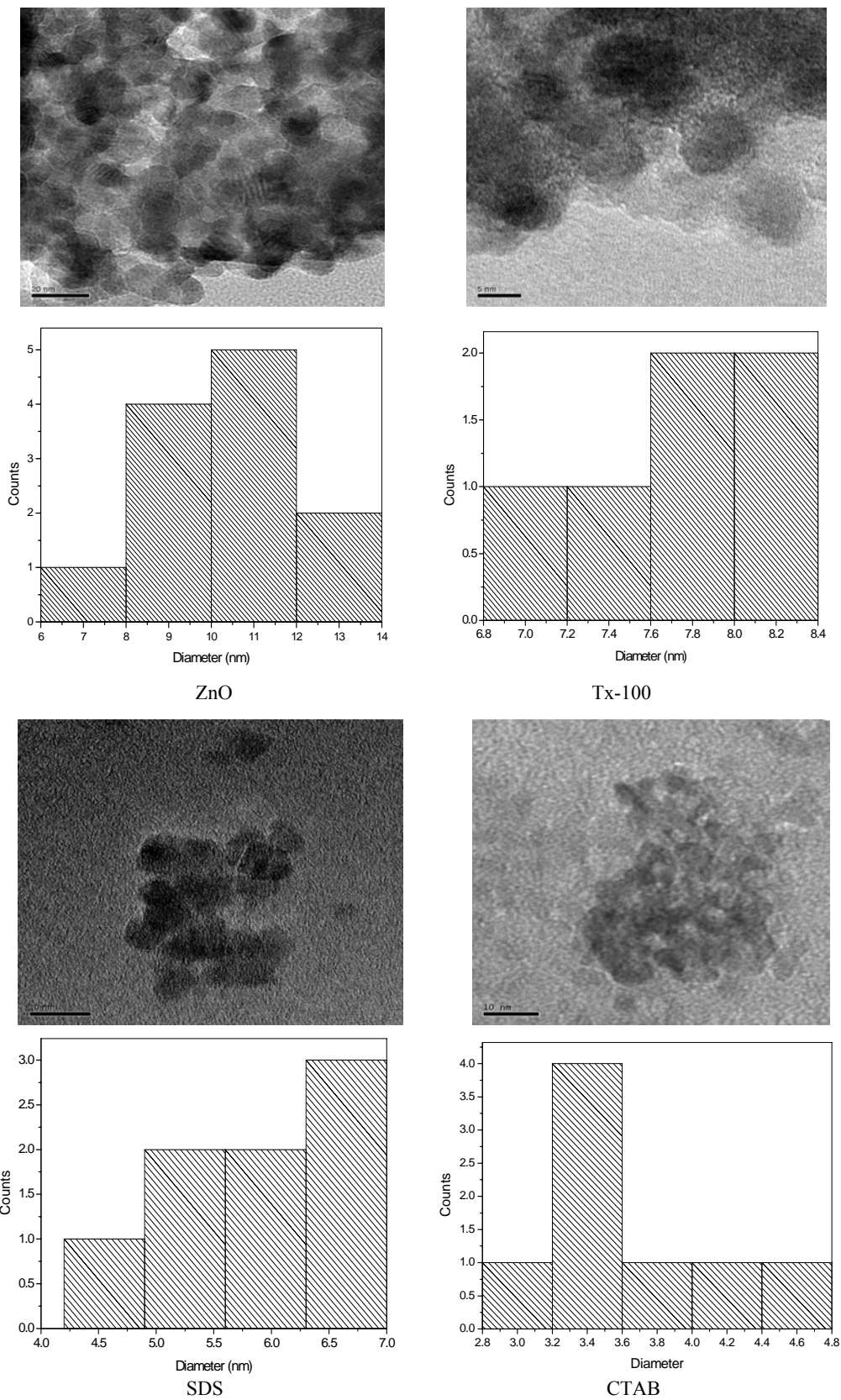


Fig. 2 HRTEM micrographs and histogram of the products grown in the solutions with various additives

3.2 Optical properties

The affect of surfactants on the optical properties of the ZnO nanomaterials was studied by UV-vis spectroscopy. The exciton absorption corresponding to ZnO, Tx-100, SDS and CTAB samples are obtained at 352, 351, 342 and 340 nm, respectively (Fig. 3). Band gaps 3.53, 3.54, 3.63 and 3.65 eV were obtained for these samples, respectively. A significant blueshift in the excitonic absorption, for nanoparticles prepared in the presence of surfactants SDS and CTAB compared to that of the ZnO nanoparticles. In our case, high efficient UV emission near band edge is attributed to the free exciton emission with high electronic density of states^[20], which shift to higher energies from 3.53 to 3.65 eV as the particle size decreases from 11 nm to 3.4 nm. In this study, the ZnO crystal grown in the SDS solution has no significant effect on UV spectra of ZnO nanoparticles.

The dependence of particle size on the optical absorption energy can be expressed based on an effective mass approximation^[21] as following equation.

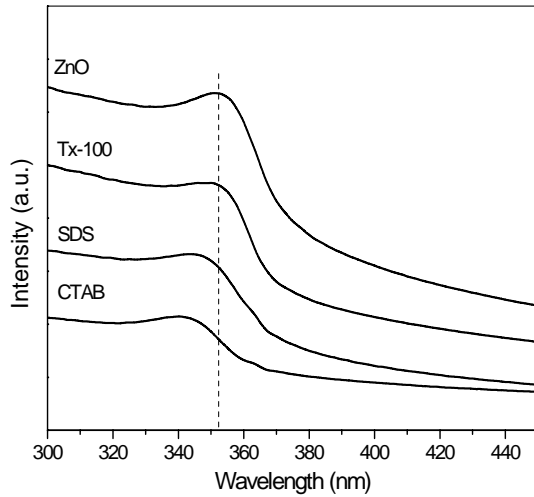


Fig. 3 UV-vis spectral of the products grown in the solutions with various additives

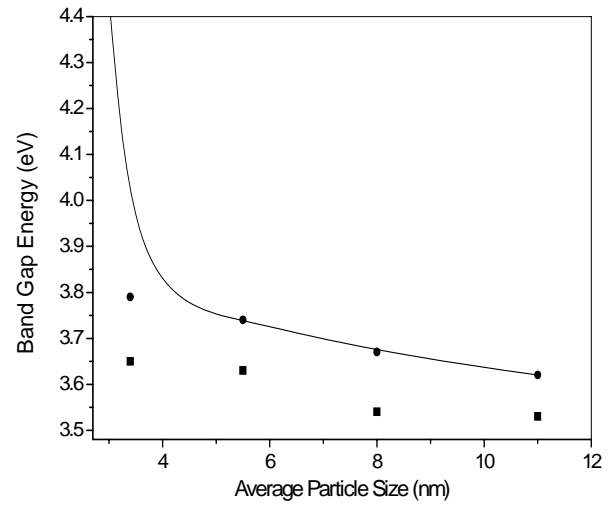


Fig. 4 Variation of the absorption band gap (●) and emission energy (■) of the ZnO nanoparticles as a function of the average particles size

Note: The solid line is the determined by the effect mass model from Eq. 1.

$$E_g \cong E_g^{\text{bulk}} + \frac{\hbar^2 \pi^2}{2er^2} \left(\frac{1}{m_e m_0} + \frac{1}{m_h m_0} \right) - \frac{1.8e}{4\pi\epsilon\epsilon_0 r} - \frac{0.124e^3}{\hbar^2 (4\pi\epsilon\epsilon_0)^2} \left(\frac{1}{m_e m_0} + \frac{1}{m_h m_0} \right)^{-1} \quad (1)$$

Where E_g^{bulk} is the bulk band gap (eV), \hbar is Planck's constant, r is the particle radius, m_e is the electron effective mass, m_h is the hole effective mass, m_0 is the free electron mass, e is the charge on the electron, ϵ is the relative permittivity, and ϵ_0 is the permittivity of free space. Fig. 4 shows the band versus particle radius calculated using Eq. (1). The band gap was decreased by increasing the particle radius. Generally, it is accepted in ZnO $E_g^{\text{bulk}} = 3.34$ eV, $m_e = 0.26$ and $m_h = 0.59$ ^[22-23]. From the experimental results, energy gap with $E_g^{\text{bulk}} = 3.53$ eV was found to be the lowest energy gap for our ZnO nanoparticles. Therefore, $E_g^{\text{bulk}} = 3.53$ eV was adopted from the lowest onset energy gap for in the current study. The effect of the particle size on calculated band gap energy from Eq. 1 is shown as the solid line. The onset absorption is very consistent with the calculated band gap energy. The experimental results obtained from the optical absorption spectra and the HR-TEM images

conducted in this study are consistent with the above theoretical calculations. This further validates the excellent correlation among the optical properties, the bandgap energies, and the sizes of our ZnO nanoparticles. This Stokes shift increases as the particle size decreases and has been observed in other II–VI and III–V nanoparticles (e.g., InP, CdSe) and extrapolated exponentially or hyperbolically^[24]. Such a presentation was previously reported as either size-dependent electron-phonon processes or size-dependent spin-orbit exchange interaction, which may contribute to the Stokes shift.

Medium of reaction play an important role in the growth rate of ZnO nanoparticles. It is well known that aqueous surfactant solution above CMC is a homogeneous mixture of polar and non-polar groups and two pseudophases of different polarities are formed. The zinc acetate precursor was first distributed between the aqueous and micellar pseudophases, then removal of the intercalated acetate ions to form the highly polar active complex intermediate $[Zn(OH)_n]^{2-n}$. In case of CTAB solution, the zinc acetate molecules come closer to the micellar head group region (positively charged ammonium groups) due to the electrostatic interactions between the head groups of cationic micelles and negatively charged acetate groups of zinc acetate which assist in localization of the zinc acetate precursor on the micellar surface. At the same time the micellar surface is the preferred reaction site for the formation of the highly polar intermediate $[Zn(OH)_n]^{2-n}$ due to the highly polarity of micellar surface. On the other hand, the formation of $[Zn(OH)_n]^{2-n}$ takes place in aqueous phase when anionic surfactant (SDS) or nonionic surfactants (Tx-100) are utilized as a reaction media, because of the electrostatic repulsion between the negatively charged head group of SDS micelles or the electron pair of the head group of (Tx-100) micelles and the negatively charged acetate groups of the precursor. It means that the micellar surface efficiently stabilize $[Zn(OH)_n]^{2-n}$ which brings smaller size ZnO nanoparticles are related to their size. If so, we would

expect the spectra of ZnO colloid that prepared in presence of surfactants possess a blue shift with respect to that in absence of surfactant and the blue shift is more significant in case of CTAB media as shown in Fig. 3, implying lower particle size of ZnO.

4. Conclusions

The wurtzite ZnO nanoparticles were prepared in the aqueous solutions with additives of Tx-100, SDS and CTAB. HRTEM micrographs of all samples are showed nearly spherical nanoparticles with average particle size of 3.4-11 nm. Quantum-size effects are evident from the optical absorption spectra, which showed blue shift in the excitonic feature as compared to the bulk ZnO. The particle size calculations from the absorption edge showed that ZnO is grown nanoparticle with CTAB has smallest particle size and lowest Stokes shift.

References:

- [1] Durian P., Capel F., Tartaj J., et al. A strategic two-stage low-temperature thermal processing leading to fully dense and fine-grained doped-ZnO varistors. *Adv. Mater.*, 2002, 14: 137-141.
- [2] Bauer C., Boschloo G., Mukhtar E., et al. Electron injection and recombination in Ru(dcbpy)₂(NCS)₂ sensitized nanostructured ZnO. *J. Phys. Chem. B*, 2001, 105: 5585-5588.
- [3] ZHANG X. T., LIU L. G., ZHANG L. G., et al. Structure and optically pumped lasing from nanocrystalline ZnO thin films prepared by thermal oxidation of ZnS thin films. *J. Appl. Phys.*, 2002, 92: 3293-3296.
- [4] Johnson J. C., Yan C. H., Schaller R. D., et al. Single nanowires lasers. *J. Phys. Chem. B*, 2001, 105: 11387.
- [5] Pillai S. C., Kelly J. M., McCormack D. E., et al. Self-assembled arrays of ZnO nanoparticles and their application as varistor materials. *J. Mater. Chem.*, 2004, 14: 1572-1578.
- [6] Seelig E. W., TANG B., Yamilov A., et al. Self-assembled 3D photonic crystals from ZnO colloidal spheres. *Mater. Chem. Phys.*, 2003, 80: 257-261.
- [7] Hoyer P. and Weller H.. Potential-dependent electron injection in nanoporous colloidal ZnO films. *J. Phys. Chem. B*, 1995, 99: 14096-14100.
- [8] Van Dijken A., Meulenkaamp E. A., Vanmakekelbergh D., et al. The luminescence of nanocrystalline ZnO particles: The mechanism of the ultraviolet and visible emission. *The J. Lumin.*, 2000, 87-89: 454-456.
- [9] Mondelaers D., Vanhoyland G., Van den Rul G. H., et al. Synthesis of ZnO nanopowder via an aqueous acetate-citrate gelation method. *Mater. Res. Bull.*, 2002, 37: 901-914.

- [10] Singhal M., Chhabra V., Kang P., et al. Synthesis of ZnO nanoparticles for varistor application using Zn-submitted aerosol of microemulsion. *Mater. Res. Bull.*, 1997, 32: 239-247.
- [11] Tsuzuki T. and McCormick P. G.. ZnO nanoparticles synthesised by mechanochemical processing. *Scripta Mater.*, 2001, 44: 1731-1734.
- [12] Okuyama K. and Lenggoro I. W.. Preparation of nanoparticle via spray route (plenary paper). *Chem. Eng. Sci.*, 2003, 58: 537-547.
- [13] Rataboul F., Nayral C., Casanove M. J., et al. Synthesis and characterization of monodisperse zinc and zinc oxide nanoparticles from the organometallic precursor $[Zn(C_6H_{11})_2]$. *J. Chem.*, 2002, 643/644: 307-312.
- [14] Sato T., Tanigaki T., Suzuki H., et al. Structure and optical spectrum of ZnO nanoparticles produced in RF plasma. *J. Cryst. Growth*, 2003, 255: 313-316.
- [15] Viswanathan R., Lilly G. D., Gale W. F., et al. Formation of Zinc oxide-titanium dioxide composite nanoparticles in supercritical water. *Ind. Eng. Chem. Res.*, 2003, 42: 5535-5540.
- [16] Koh Y. W., Lin W. M., Tan C. K., et al. Self-assembly and selected area growth of zinc oxide nanorods on any surface promoted by an aluminum precoat. *J. Phys. Chem. B*, 2004, 108: 11419-11425.
- [17] LIU B. and ZENG H. C.. Hydrothermal synthesis of ZnO nanorods in the diameter regime of 50 nm. *J. Am. Chem. Soc.*, 2003, 125: 4430-4431.
- [18] WANG J. M. and GAO L. Synthesis and characterization of ZnO nanoparticles assembled in one-dimensional order. *Inorg. Chem. Commun.*, 2003, 6: 877-881.
- [19] Kim J. H., Choi W. C., Kim H. Y., et al. Preparation of mono-dispersed mixed metal oxide micro hollow spheres by homogeneous precipitation in a micro precipitator. *Powder Technol.*, 2005, 153: 166-175.
- [20] Kuo-Feng Lin, Hsin-Ming Cheng, Hsu-Cheng Hsu, et al. Band gap variation of size-controlled ZnO quantum dots synthesized by sol-gel method. *Chemical Physics Letters*, 2005, 409: 208-211.
- [21] SHAN F. K. and YU Y. S.. Band gap energy pure and Al doped ZnO thin films. *J. Eur. Ceram. Soc.*, 2004, 24: 1869-1872.
- [22] Brus L. E.. Electronic wave functions in semiconductor clusters: Experiment and theory. *J. Phys. Chem.*, 1986, 90(12): 2555-2560.
- [23] Shionoya S., Yen W. M. (Eds.). *Phosphor Handbook*. CRC, Boca Raton, FL, 1998.
- [24] FU H. and Zunger A.. InP quantum dots: Electronic structure, surface effects and the red-shifted emission. *Phys. Rev. B*, 1997, 56: 1496-1508.
- [25] Pesika N. S., Stebe K. J. and Searson P. C.. Determination of the particle size distribution of quantum nanocrystals from absorbance spectra. *Adv. Mater.*, 2003, 15: 1289-1291.

(Edited by Malik L. and Taylor C.)

(continued from Page 37)

- [8] Dvorak H. F., Harvey V. S. and Donagh M.. Quantification of fibrinogen influx and fibrin deposition and turnover in line 1 and 10 guinea pig carcinomas. *J. Cancer Res.*, 1984, 44: 3348.
- [9] ZHANG Y., DENG Y., Luther T., et al. Tissue factor controls the balance of angiogenic and antiangiogenic properties of tumor cells in mice. *J. Clin. Invest.*, 1994, 94(3): 1320-1327.
- [10] Min H. Y., Doyle L. V., Vitt C. R., et al. Receptor antagonists inhibit angiogenesis and primary tumor growth in syngeneic mice. *Cancer Res.*, 1996, 56(10): 248-2433.
- [11] Thompson W. D., Stirr C. M., Melvin W. T., et al. Plasmin, fibrin degradation and angiogenesis. *Nature Med.*, 1997, 2: 493.
- [12] Baserga A. and Zavagli G.. Ferrara's stem cells: An historical review on hemocytoblasts and hemohistioblasts. *Blood Cells*, 1981, 7: 537-545.
- [13] Releaven J. and Barrett J.. Introduction to bone marrow transplantation. In: Treleaven J. and Barrett J. (Eds.). *Bone Marrow Transplantation in Practice*. Churchill Livingstone. New York, USA. 1992, 3-9.
- [14] Maximilian D., Robert W. C., Neethan A. L., et al. Association of reactive oxygen species levels and radioresistance in cancer stem cells. *Nature*, advance online publication, February 4th, 2009.
- [15] Korkaya H., Paulson A., Iovino F., et al. HER2 regulates the mammary stem/progenitor cell population driving tumorigenesis and invasion. *Oncogene*, 2008, 16: 6120-6130.
- [16] Al-Hajj M., Wicha M. S., Benito-Hernandez A. M., et al. Prospective identification of tumorigenic breast cancer cells. *Proc Natl Acad Sci USA.*, 2003, 100: 3983-3988.
- [17] Siddiqui F., Amirkhosravi A., Amaya M., et al. Hemoglobin enhances tissue factor expression on human malignant cells. *Blood Coagulation and Fibrinolysis*, 2001, 12: 171-177.
- [18] Binnig G., Gerber C., Stoll E., et al. Atomic resolution with atomic force microscope. *Euro. Physics Letter*, 1997, 3: 1281-1286.
- [19] Panessa-Warren B. J. and Warren J. B.. Determining biological fine structure by differential absorption of soft x-rays. *New York Academy of Science*, 1980, 342: 350-367.

(Edited by Malik L. and Taylor C.)